AD-A169 349 MODELS AND RADIATION OF RAILGUN PLASMA ARMATURES WITH NON-IDEAL PLASMA PR..(U) WESTINGHOUSE RESEARCH AND DEVELOPMENT CENTER PITTSBURGH PA Y C THIO ET AL. 1/1

UNCLASSIFIED 30 MAY 86 ARO-20115.2-EG DAAG29-83-C-0030 F/G 20/7 NL

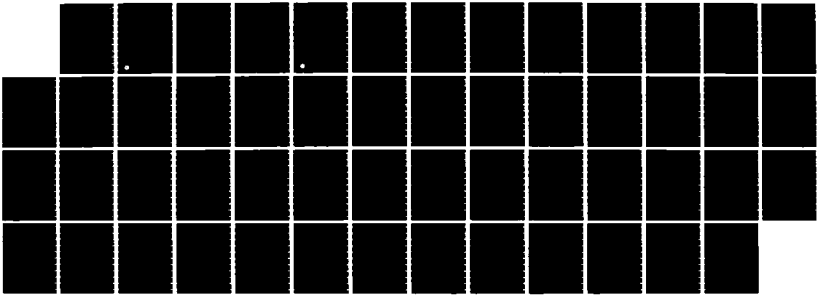

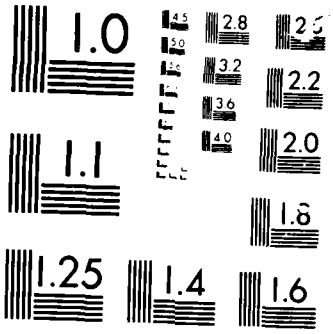
1.0
1.1
1.25
1.4
1.6
1.8
2.0
2.2
2.8
3.2
3.6
4.0
4.5
5.0

MODELS AND RADIATION OF RAILGUN PLASMA ARMATURES WITH NON-IDEAL PLASMA PROPERTIES

FINAL REPORT

Y. Chia Thio, L. S. Frost

May 30, 1986

U.S. Army Research Office
Research Triangle Park
North Carolina

Contract No. DAAG29-83-C-0030

APPROVED FOR PUBLIC RELEASE
DISTRIBUTION UNLIMITED

Westinghouse R&D Center
1310 Beulah Road
Pittsburgh, Pennsylvania 15235

UNCLASSIFIED

SECURITY CLASSIFICATION OF THIS PAGE (When Data Entered)

REPORT DOCUMENTATION PAGE

READ INSTRUCTIONS BEFORE COMPLETING FORM

1. REPORT NUMBER: ARO 20115.2-EG	2. GOVT ACCESSION NO.: AD-A169 349 N/A
3. RECIPIENT'S CATALOG NUMBER: N/A	
4. TITLE (and Subtitle): MODELS AND RADIATION OF RAILGUN PLASMA ARMATURES WITH NON-IDEAL PLASMA PROPERTIES	5. TYPE OF REPORT & PERIOD COVERED: Final Report Oct. 1, 1983 to Sep 30, 1985
	6. PERFORMING ORG. REPORT NUMBER:
7. AUTHOR(s): Y. C. Thio and L. S. Frost	8. CONTRACT OR GRANT NUMBER(s): DAAG29-83-C-0030
9. PERFORMING ORGANIZATION NAME AND ADDRESS: Westinghouse Electric Corporation, R&D Center, 1310 Beulah Road, Pittsburgh, PA 15235	10. PROGRAM ELEMENT, PROJECT, TASK AREA & WORK UNIT NUMBERS: N/A
11. CONTROLLING OFFICE NAME AND ADDRESS: U. S. Army Research Office, Post Office Box 12211, Research Triangle Park, NC 27709	12. REPORT DATE: May 30, 1986
	13. NUMBER OF PAGES: 44
14. MONITORING AGENCY NAME & ADDRESS (if different from Controlling Office)	15. SECURITY CLASS. (of this report): Unclassified
	15a. DECLASSIFICATION/DOWNGRADING SCHEDULE

16. DISTRIBUTION STATEMENT (of this Report)

Approved for public release; distribution unlimited.

17. DISTRIBUTION STATEMENT (of the abstract entered in Block 20, if different from Report)

NA

18. SUPPLEMENTARY NOTES

The view, opinions, and/or findings contained in this report are those of the author(s) and should not be construed as an official Department of the Army position, policy, or decision, unless so designated by other documentation.

19. KEY WORDS (Continue on reverse side if necessary and identify by block number)

Plasma Armatures	Railguns	Plasma Temperature
Controlled Generation	Electromagnetic Launchers	Plasma Length
Arc Erosion	Lithium Compounds	Plasma Modeling
Rail Heating	Plasma Radiation	
Plasma Seeding	Chemical Propellants	

20. ABSTRACT (Continue on reverse side if necessary and identify by block number)

A theoretical framework for modeling the characteristics of railgun plasma armatures is developed taking into account non-ideal transport properties and equation of state. The electrical resistivity of the plasma is calculated as a sum of contributions from electron-ion and electron-neutral collisions. Non-ideal correction to the ionization potential and pressure in Saha's equation and the equation of state is included. For electron-ion resistivity,

(cont. on reverse)

DD FORM 1 JAN 73 1473 EDITION OF 1 NOV 65 IS OBSOLETE

UNCLASSIFIED

SECURITY CLASSIFICATION OF THIS PAGE (When Data Entered)

20. ABSTRACT CONTINUED

we use the basic formulation of Khalfaoui for highly non-ideal plasma, smoothed and calibrated with respect to the results of Kurilenko & Valuev, Vorobiov el al and Kovitya. For electron-neutral resistivity, we use a formulation which allows the fitting of an infinite half-power series to experimentally determined energy spectrum of electron-neutral collision frequencies for a given atom.

Next, a steady-state magneto-gasdynamic model improved over earlier works is developed. In this model, the net Lorentz force exerted on the plasma armature is exactly accounted for.

Finally, we apply the model to study the radiation emanating from the plasma armature. It is found, on the one hand, that the radiation from the plasma armature under the conditions of most railgun experiments conducted in the past is sufficiently high to cause ablation. On the other hand, the modelling results also indicate that there indeed exist domains of operating parameters in which radiative ablation of the wall materials can be completely eliminated. Whether these favorable domains of operating parameters can be realized in practice remains a development of the future, though preliminary experiments conducted in a companion program sponsored by DoE and experiments in other institutions based upon the theoretical recommendations developed here have produced significant reduction of ablation of the rails. It should be emphasized, however, that ablation mechanisms other than radiation could also be present.

MODELS AND RADIATION OF RAILGUN PLASMA ARMATURES WITH NON-IDEAL PLASMA PROPERTIES

FINAL REPORT

Y. Chia Thio, L. S. Frost

May 30, 1986

U S. Army Research Office
Research Triangle Park
North Carolina

Contract No. DAAG29-83-C-0030

A-1

Westinghouse R&D Center
1310 Beulah Road
Pittsburgh, Pennsylvania 15235

THE VIEW, OPINIONS, AND/OR FINDINGS CONTAINED IN THIS REPORT ARE THOSE OF THE AUTHOR(S) AND SHOULD NOT BE CONSTRUED AS AN OFFICIAL DEPARTMENT OF THE ARMY POSITION, POLICY, OR DECISION, UNLESS SO DESIGNATED BY OTHER DOCUMENTATION.

Table of Contents

MODELS AND RADIATION OF RAILGUM PLASMA ARMATURES WITH NON-IDEAL PLASMA PROPERTIES

Y. Chia Thio, L. S. Frost
Engineering Department

ABSTRACT

A theoretical framework for modeling the characteristics of railgun plasma armatures is developed taking into account non-ideal transport properties and equation of state. The electrical resistivity of the plasma is calculated as a sum of contributions from electron-ion and electron-neutral collisions. Non-ideal correction to the ionization potential and pressure in Saha's equation and the equation of state is included. For electron-ion resistivity, we use the basic formulation of Khalfaoui for highly non-ideal plasma, smoothed and calibrated with respect to the results of Kurilenko & Valuev, Vorobiov et al and Kovitya. For electron-neutral resistivity, we use a formulation which allows the fitting of an infinite half-power series to experimentally determined energy spectrum of electron-neutral collision frequencies for a given atom.

Next, a steady-state magneto-gasdynamic model improved over earlier works is developed. In this model, the net Lorentz force exerted on the plasma armature is exactly accounted for.

Finally, we apply the model to study the radiation emanating from the plasma armature. It is found, on the one hand, that the radiation from the plasma armature under the conditions of most railgun experiments conducted in the past is sufficiently high to cause ablation. On the other hand, the modelling results also indicate that there indeed exist domains of operating parameters in which radiative ablation of the wall materials can be completely eliminated. Whether these favorable domains of operating parameters can be realized in practice remains a development of the future, though preliminary experiments conducted in a companion program sponsored by DoE and experiments

in other institutions based upon the theoretical recommendations developed here have produced significant reduction of ablation of the rails. It should be emphasized, however that, ablation mechanisms other than radiation could also be present.

1. Introduction

Theoretical models for railgun arcs have been introduced by McNab[1], Powell and Batteh[2], Thio[3-5], Powell and Batteh[6], Powell[7] and Batteh[8]. These studies have been useful in planning plasma driven railgun experiments in recent years. They have been particularly useful in designing suitable railgun diagnostics and in the analysis of experimental data.

In these earlier works, liberal use was made of simple expressions for the plasma transport properties and the equation of state, based essentially upon ideal plasma behavior. In these studies, the plasma armatures were estimated to have rather high temperatures (30,000 K - 60,000 K) and relatively low pressures (100 MPa - 200 MPa). At these temperatures and pressures, ideal plasma behavior was a reasonable assumption, making these studies internally consistent.

Through the early experimental work of Hawke et al[9], Thio et al[10], Bedford et al[11], Clark and Bedford[12] and Bedford[13], it soon became clear that ablation of the wall materials was commonplace in railguns in which the arc was generated by exploding metallic foils of relatively low mass. This ablation adds considerable mass to the arc in a relatively short time, whence the arc begins to expand and cool leading to the formation of a relatively cool arc at high pressure. The arc evolves and enters the regime of non-ideal plasmas. Parker[14] later emphasized the important role this ablation played in degrading railgun performance.

The first objective of the work reported here is to develop the appropriate theoretical capability so that we can extend our investigation of the behavior of railgun arcs into the realm of cold, high

pressure arcs. The theoretical construct we shall develop in this paper is based upon non-ideal plasma theory.

The second objective is to introduce a refinement on the momentum equation and boundary conditions used in the earlier works. With this refinement the accelerating Lorentz force can now be accurately accounted for.

The third objective is to apply the model developed to study the radiation emanating from the plasma armature over a broad range of operating parameters in a railgun. Before the advent of this work, there were many conjectures on the question of what are the dominating physical processes responsible for ablation of the wall materials in railguns. Many of these speculations remain to-day and need to be explored. In this regard, what has been accomplished from this work is that radiation has been theoretically established as an important physical process to consider in the context of wall ablation in railguns. This does not preclude the possibility of other mechanisms being present and possibly being important or even more important. What it implies is that, if wall ablation in a railgun is to be eliminated, radiative ablation is a significant component which needs to be eliminated.

2. A MAGNETOGASDYNAMIC MODEL

Powell and Batteh[2,6-8] and Thio[3-5] have previously developed steady state or quasi-steady state 1-D models for the plasma armature. The model we shall develop in the present study shares a similar starting point with these earlier models but differs from them in several essential details. Investigations on the structure of railgun arcs have also been undertaken by Stainsby and Bedford[38] and Marshall[39,40], in which the fine structure of the armature is emphasized, especially in the boundary layer near the wall. Our study here focuses on the interior of the arc (the arc column) sufficiently far away from the wall so that the arc may be reasonably considered as a continuum. The boundary layer between the wall and the arc column is not considered here.

Figure 1 shows the geometry of the model. The axes are chosen so that the z-axis is in the direction of projectile travel, the y-axis is normal to the rails, and the x-axis is horizontal into the paper. We assume that all physical variables can vary at most in the z-direction (1-D) and that the entire system comprising the plasma armature and the projectile has reached a steady state and moves at a constant acceleration driven by a constant total current. The momentum equation for the plasma armature in that case can be written as:

$$\frac{dp}{dz} + \rho a = jB \tag{2}$$

where p is the gas pressure, ρ is the gas density, a is the acceleration of the entire system, j is the current density and B is the magnetic field. Ampere's law takes the simple form,

$$\frac{dB}{dz} = -\mu j \tag{3}$$

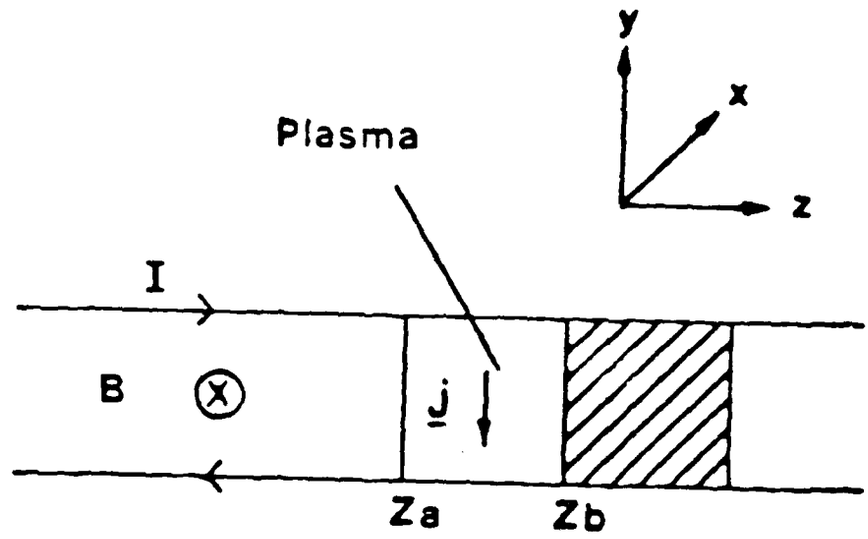

Figure 1 — Geometry of the plasma model.

where μ ($4\pi \times 10^{-7}$H/m) is the permeability of free space. We require an equation of state to relate the pressure to the density. The ideal gas equation of state was used in the earlier models of Thio, Powell and Batteh. Herein we introduce the non-ideal gas pressure as a perturbation on the ideal gas pressure, and write the equation of state in the form,

$$p = \{1 + \sum_{i=1}^{\infty} \alpha_i Z_i + g(\gamma/\bar{Z})\} \frac{\rho k_B T}{m_p} \qquad (4)$$

where $g(\gamma/\bar{Z})$ is a slowly varying function of the non-ideal parameter $\gamma/\bar{Z}$ (see expression (18)), and represents the non-ideal perturbation to the true pressure, α_i is the ionization fraction of the ion in the i-th

and cannot be accurately approximated by 1-D analysis without some modifications to take account of the 3-D effects. In particular, the field at the forward boundary of the plasma armature is not zero.

These reasonings led Thio[3,4] originally to suggest an alternative approach. While accepting the fact that Maxwell's equations in 1-D require that the boundary magnetic field should equal its value at infinity, Thio decided to discard the requirement that the field at the forward boundary B_a must be zero. This opens up precisely the needed degree of freedom necessary to obtain a better estimate for the unknown magnetic field B_b at the rear boundary. In Thio[4], the rear boundary magnetic field was obtained by actually averaging the field across the mid-line of the bore in between the rails produced by the current flowing in the finite-height rails and in the plasma. The rails were assumed to be infinitely long and the rail current was assumed to flow only on the inner rail surface. The method gives a much better estimate of the accelerating force, typically within 20% of the true value. Batteh[8] later improves on this model by averaging the field across the bore of the gun, not only for the field at the rear boundary, but also for each arc cross-section (x-y plane) normal to the z-direction. In doing so, Batteh obtained a much improved momentum equation for the arc, but sacrificed much of the simplicity of the 1-D approach. The resultant equation was an integro-differential equation.

In this paper, we suggest yet another approach which is designed to give exactly the correct value of the Lorentz force without sacrificing the mathematical simplicity of the 1-D approach, and at the same time retaining strict consistency with Maxwell's equations in 1-D.

We begin with the expression for the Lorentz force given globally from field theoretic consideration in the form,

$$F_L(t) = \frac{1}{2} L_r'(t)\ I_r^2(t) + M_{12}'(t)\ I_a(t)\ I_r(t) \qquad (11)$$

where $I_r(t)$ is the current flowing in the inner rails and I_a is the current flowing in the augmentation windings, L'_r is the inductance gradient of the inner rails, M'_{12} is the mutual inductance gradient between the inner rails and the augmentation windings. The values of the inductance gradients L'_r and M'_{12} pertaining to a specific application can be accurately obtained either by an actual measurement with an LCR meter on a given gun or by computation using a 2-D or 3-D EM field analysis code (Patch et al[15], Thio et al[16]). The magnetic fields at the rear and forward boundary are now chosen to satisfy (8), (9) and the exact value of the Lorentz force (11). The results are,

$$B_a(t) = \left(\frac{h\, L'_{eff}(t)}{2\mu w} + \frac{1}{2}\right) \frac{\mu\, I_r(t)}{h} \tag{12}$$

$$B_b(t) = \left(\frac{h\, L'_{eff}(t)}{2\mu w} - \frac{1}{2}\right) \frac{\mu\, I_r(t)}{h} \tag{13}$$

where,

$$L'_{eff}(t) = L'_r + 2\,[I_a(t)/I_r(t)]\, M'_{12} \tag{14}$$

is an effective inductance gradient for the system comprising the inner rails and the augmentation winding.

The resultant model not only is capable of including effects of flux augmentation (series or trans-augmentation), it is also ideally suitable for modeling non-steady-state behavior of plasma armatures subject to time-varying current and time-varying rail inductance gradient. For this purpose, time dependence has been explicitly indicated in the above expressions.

We need an equation for the temperature T of the plasma armature. The temperature is determined by the radiative equilibrium of

state of ionization, k_B is the Boltzmann constant (1.38×10^{-23} J/deg K) and m_p is the mass of the atomic species (A.W. $\times$ 1.66×10^{-27}kg). A brief discussion on the non-ideal perturbation term in this equation is given later in Section 4.

For a uniform current and temperature distribution within the arc, the above set of equations can be solved analytically, provided we treat the non-ideal function g as a constant parameter. The solution yields the pressure distribution within the arc to be,

$$p\ (Z) = \frac{\mu_j^2}{(k_1 a)^2}\ \{b_1\ (1 - e^{-k_1 a \varsigma}) - k_1 a \varsigma\} \tag{5}$$

where,

$$b_1 = \frac{B\ (Z_a)\ k_1 a}{\mu_j} + 1$$

$$k_1 = \frac{m_p}{\{1 + \sum_{i=1}^{\infty} \alpha_i Z_i + g(\gamma/\bar{Z})\}\ k_B T}$$

and $\varsigma = z - z_a$, z_a is the z-coordinate of the rear boundary of the plasma armature. Using the equation of state (4), the density distribution can be determined from (5), and the total mass for the plasma armature can be obtained as,

$$m_A = (\frac{\mu w}{ah})\ (\frac{b_2}{b_3})\ T^{-1}\ I_p^2 \tag{6}$$

where,

$$b_2 = \frac{1}{(k_1 a l)^2}\ \{ab_1\ [1 + \frac{1}{k_1 a l}\ (e^{-k_1 a l} - 1)] - k_1 a l\}$$

$$b_3 = \{1 + \sum_{i=1}^{\infty} \alpha_i Z_i + g(\gamma/\bar{Z})\}\ \frac{k_B}{m_p} \tag{7}$$

In both the expressions for the pressure distribution and the total armature mass, the magnetic field $B_a = B(z_a)$ at the rear boundary enters as a parameter and needs to be determined.

Equation (3) expressing Ampere's law requires that the fields at the rear and the forward boundaries be connected by the relationship,

$$B(z_b) - B(z_a) = \frac{\mu I_r}{h} \tag{8}$$

where I_r is the total current flowing through the plasma armature, and h is the bore height (the height of that portion of the rails from which the arc collects its current). Also, the net Lorentz force exerting on the plasma armature as a whole is rigorously given by the volume integral of j x B, which from the 1-D Maxwell's equations gives

$$F_L = \frac{A}{2\mu} (B_b^2 - B_a^2) \tag{9}$$

In Powell and Batteh[2], the forward boundary magnetic field was set to zero. The rear boundary magnetic field B_b follows from expression (8). Upon substituting this boundary magnetic field into expression (9), Powell and Batteh[2] obtained for the net Lorentz force,

$$F_L = \frac{1}{2} \left(\frac{\mu w}{h}\right) I_r^2 \tag{10}$$

While the procedure can be shown to be rigorously correct for the case of a true 1-D geometry in which the rails are infinitely high, it tends to overestimate the net acceleration, typically by a factor of 2 or more. As can be seen from (10), the equivalent rail inductance gradient L' is μ (1.257 μH/m) for the case of a square-bore railgun (w=h), whereas in practice the actual value of L' for a square-bore railgun is typically 0.3 - 0.4 μH/m.

The basic cause of this discrepancy is that the magnetic field near the boundaries of the plasma armature is essentially 3-D in nature

the plasma armature. The ohmic dissipation in the plasma armature is balanced exactly by the radiative loss from the arc to the side walls and through the front and the rear boundaries,

$$I_r^2 R_A = \sigma_s T^4 (2 \epsilon_r hl + 2 \epsilon_i wl + \epsilon_a wh + \epsilon_b wh) \qquad (16)$$

where R_A is the net resistance of the plasma armature, and we have allowed an emissivity ϵ_r for radiation to the rails, a separate emissivity ϵ_i for radiation to the insulator, and an emissivity ϵ_a for radiation through the rear boundary, and another emissivity ϵ_b through the forward boundary. The plasma resistance is calculated from the expression,

$$R_A = \frac{\eta_p w}{hl} \qquad (17)$$

where l is the length of the plasma armature, h is the height of the bore, w is the width of the bore (separation between the rails), and η_p is the mean resistivity of the plasma armature.

To make further progress, we need expressions which would give reasonable estimates of the plasma resistivity and emissivity.

3. RESISTIVITY OF RAILGUN PLASMA ARMATURES

In the search for optimum plasma armatures to avoid the ablation problems of the early railguns, we were led gradually but steadily to the realm of plasmas which exhibit strongly non-ideal behavior.

For most of the plasmas considered in the present study, significant ionization is present. The degree of ionization is typically in excess of 20%. In these plasmas, the deviation from ideal behavior arises mainly from the collective electrostatic interactions among the charged and neutral particles, in opposition to the randomizing effect of their thermal energy. The ratio of the mean coulombic energy of interaction of the particles to their mean thermal energy,

$$\gamma = \frac{\bar{Z}\, e^2\, n_c^{1/3}}{4\,\pi\,\epsilon_o\, k_B\, T} \tag{18}$$

where e is the electronic charge, $\bar{Z}$ is the effective charge of the ions, and n_c is the density of all charged particles, is a good indicator of the severity of the non-ideal behavior. Note that we have used the density of all charged particles including electrons in the definition of γ rather than the more common practice of using only the electron density n_e. The higher the value of the non-ideal parameter γ, the greater is the deviation from ideal behavior. Generally, ideal plasma theory is applicable only when $\gamma \ll 0.1$. For values of $\gamma > 0.1$, non-ideal plasma theory is required. At a fixed temperature, the degree of non-ideal behavior increases as the electron density increases. For electron density below the critical density,

$$\bar{n} = 2\ (2\ \pi\ m_e\ k_B\ T)^{3/2}/h^3 \qquad (19)$$

where m_e is the electron mass (9.11×10^{-31}kg) and h is the Planck constant (6.624×10^{-34}ns), the electron energy distribution in the plasma remains essentially classical in accordance with the Maxwellian energy distribution. Beyond the critical density, the electron energy distribution becomes non-Maxwellian and is governed by Fermi statistics with the gas then becoming a quantum plasma[18].

In this study, our computations are limited to classical non-ideal plasmas. Most of the plasmas we examined have density at least a factor of 5 below the critical density, though some come as close as within a factor of 2 of the critical density, when the validity of the classical Maxwellian distribution becomes questionable. We have not extended our search for plasma armatures into the domain of quantum plasmas. There is, however, no apriori reason for not doing so.

Currently an active area of research, the work on the characterization of non-ideal plasmas has produced voluminous collections of largely unsystematized experimental data and a great variety of theoretical approaches. We make no claim to the complete coverage of available literature and results on the subject. A good review of the subject of electrical transport properties for these plasmas can be found in the works of Khalfaoui[17] and others[18-21].

The electrical resistivity η_T of a classical plasma is the result of all the collisions among all the particles present, and can be given in terms of the collision frequencies or equivalently the relaxation times of the various species of particles by,

$$\eta_T = \frac{m_e}{n_e e^2}\ \{\langle \nu_{en} \rangle + \langle \nu_{ei} \rangle\} \qquad (20)$$

where ν_{en} and ν_{ei} are the collision frequencies of electrons with neutral particles, and ions respectively, and their mean values indicated by the brackets < > has been taken with respect to the normalized Maxwellian energy distribution,

$$f(E) = 2\,\pi^{-1/2}\,(kT)^{-3/2}\,E^{1/2}\,\exp\,(-E/k_BT) \qquad (21)$$

3.1 COULOMBIC RESISTIVITY

For the contribution to the resistivity from the interaction of charged particles with charged particles, we based our calculation mainly on the theory of Khalfaoui[18] who gives a comprehensive model covering both the non-ideal classical and quantum plasmas. For much of the domain of our computation, we find that the Khalfaoui resistivity shows only a weak dependence on the non-ideal parameter γ/Z, and can be reasonably approximated by the following simple expression,

$$\eta_{ei} = 3.5 \times 10^2\,S_T\,\exp\,(-2\gamma/3\bar{Z})\,T^{-3/2} \qquad (23)$$

showing clearly the predominant 3/2- power dependence on the temperature.

Despite the 3/2-power law of the temperature, the difference between expression (23) and Spitzer's resistivity in functional form and numerical values is fundamental and significant. Spitzer's resistivity involves a logarithmic dependence on the ratio of the Debye length L_D to the impact parameter p_0 where πp_0^2 plays the role of a scattering cross-section. This arises from setting the Debye length as the cut-off distance for coulombic interaction in approximating the relaxation times of electron-ion encounters in deriving Spitzer's resistivity. The approximation makes sense so long as there is a sufficiently great number of particles within the Debye sphere (radius L_D) to shield the nuclear charge of the ion from outside the Debye sphere, so that nearly all the electron-ion encounters take place within the Debye sphere. However, at sufficiently high electron density, due to the long range

nature of the electrostatic interaction, a significantly large amount of coulombic scattering occurs outside the Debye sphere. This is reflected numerically in the value of the scattering radius p_0 being similar in magnitude or greater than the Debye radius ($\Lambda \leq 1$). The Debye length can no longer serve as the cut-off distance in evaluating the relaxation time integral. Consequently, Spitzer's expression for the resistivity fails.

In the range of particle density and temperature relevant to our present study, we have found that Spitzer's expression can underestimate the coulombic resistivity by as much as a factor of 5 compared with expression (23).

3.2 THE ELECTON-NEUTRAL SCATTERING RESISTIVITY

As the plasmas under consideration are not fully ionized, a significant number of collisions could occur between the electrons and the neutral particles. Their contribution η_{en} to the overall resistivity should therefore be appropriately taken into account,

$$\eta_{en} = \frac{m_e}{n_e e^2} \langle \nu_{en} \rangle \tag{24}$$

The principal difficulty here is the evaluation of the mean electron-neutral collision frequency. The theoretical problem consists of solving the Schrodinger's equation for the scattering of electrons by a many-electron atom, calculating the phase shift and evaluating the scattering cross-section using the standard phase shift formula[33]. We shall not follow that procedure here. Instead, we shall make use of empirical expressions for the dependence of the collisional frequency on electron energy deduced from actual experimental measurements.

For the gaseous atoms of interest, we have found it possible to approximate the energy dependence of the collisional frequency between the electrons and atoms within experimental limits of scatter and

discrepancy using the following functional form:

$$\nu_{en} = n_n \sum_{i=0}^{\infty} b_i E^{i/2} \tag{25}$$

where the $b'_i s$ are coefficients chosen to best fit the experimental data, E is the electron energy in J and n_n is the number density of the neutral particles present in m^{-3}. Taking the average with the Maxwellian energy distribution (21), the contribution to the plasma resistivity from the electron-atom scattering is computed in the form,

$$\eta_{en} = g_{en} T^{-3/2} \tag{26}$$

where the function g_{en} is given by,

$$g_{en} = \left(\frac{m_e}{e^2}\right) \left(\frac{1 - \sum_{i=1}^{\infty} \alpha_i}{\sum_{i=1}^{\infty} \alpha_i Z_i}\right) T^2 \sum_{j=-1}^{\infty} s_j T^{1/2}$$

Using the data from Frost[23] and Cambel[24], a table of values for the various coefficients and atoms have been compiled as shown in Table 1 and used in this study.

Before we can use the results of this section, the degree of ionization which determines the densities of the charged species at a given temperature and pressure needs to be determined. For this purpose, we need an equation of state and an expression giving the effective ionization potential for the atomic species under non-ideal conditions.

Table 1. The Coefficients s_j for the Function g_{en}

	s_o 10^{-15}	s_1 10^{-17}	s_2 10^{-20}	s_3 10^{-22}	s_4 10^{-24}
O	0.57	0	0	0	0
H	4.4	-1.8	8.5	-4.4	2.4
N	1.25	0	0	0	0
C	0.95	0	0	0	0
hi	6.2	0	0	0	0

4. THE NON-IDEAL EQUATION OF STATE

The equation of state for high density matter has been a subject of extensive research for the last fifty years. Computational methods have grown steadily from relatively simple models to highly sophisticated, complicated ones. The starting point in most of these methods is a model for the potential of the atom in a given ionization state. Through this potential, charged and neutral particles collectively or individually interact. The Helmholtz free energy associated with this interaction is derived, from which the equation of state is determined. Recent work includes those of Liberman[25], Kerley & Abdallah[26], and Rinker[27] etc. More historical work includes those of Cowan & Ashkin[28] using the Thomas-Fermi-Dirac model of the atom. Extensive tabulations of the equation of state for a great number of elements over a wide range of pressures and temperatures can be obtained from the library of SESAME[29].

A related effect is the lowering of the ionization energy, a subject which by itself has attracted many investigators and is richly endowed with literature[30-34].

The detailed, accurate quantum dynamical computations of the equation of state is beyond the scope of this study, nor is it required. In the present context, the pertinent effect due to non-ideal behavior of the plasma is a small reduction in the gas pressure and ionization energy due to the attractive electrostatic interaction between the charged particles. A reasonable estimate for these corrections could be obtained using classical or semi-classical methods.

In the realm of classical or semi-classical methods, a variety of theoretical results are available. Thus, for a weakly non-ideal

plasma this pressure reduction has been calculated within the framework of the Debye-Huckel theory (see for example Landau & Lifshitz[34] or Zel'Dovich & Raizer[35] p. 216). That theory requires that there are sufficient number of particles within the Debye sphere to justify the statistical treatment on which the Debye-Huckel theory is based. As the electron density increases, the mean number of particles within the Debye sphere decreases to below unity, at which point the Debye-Huckel theory completely loses its physical meaning. This corresponds approximately to values of $\gamma > 0\ 1$. Unsold in 1948[30] introduced the so-called 1-particle theory, which was analysed later by Ecker & Kroll[31] to make physical sense only for very high density, typically for $\gamma >> 1$. Even in that range, Ecker & Kroll had found that Unsold's result could give unrealistically high estimates for the coulombic interaction energy, which is reflected in an excessive lowering of the ionization potential. Ecker and Kroll[31] attempted a smoothing of the results of these two diverse approaches. A unification of these classical theories based on a refinement of the theory of Ecker and Kroll is recently given by Thio[36]. For our immediate purpose, we shall adopt the model formulated in Thio[36], which gives simultaneously an expression for the pressure correction and the lowering of the ionization energy.

Thio[36] gives the pressure correction for a non-ideal plasma over the full range of the non-ideal parameter γ from 0 to approximately 1 as,

$$\Delta p = - \frac{e^2}{24 \pi \epsilon_o (L_D + r_o)} \sum_{i=1}^{\infty} n_i Z_i (1 + Z_i) \qquad (27)$$

where L_D is the Debye radius which is given by,

$$L_D = \left[\frac{e^2}{4 \pi \epsilon_o k_B T} \sum_{i=1}^{\infty} n_i Z_i (1 + Z_i)\right]^{-1/2}$$

and r_o is the mean interparticle separation for the charged particles, defined as:

$$r_o = (\frac{4\pi}{3} n_c)^{-1/3} = (\frac{4\pi}{3} \sum_{i=1}^{\infty} (1 + Z_i)\ n_i)^{-1/3}$$

In the above expressions, n_i denotes the number density of the ith ionic species, and Z_i the ionic charge in units of electronic charge ($Z_i = i$).

Combining the pressure correction with the ideal gas pressure, we may write the equation of state as,

$$p = [1 + \sum_{i=1}^{\infty} \alpha_i Z_i + g(\gamma/\bar{Z})]\ \frac{\rho\ k_B\ T}{m_p} \tag{28}$$

where the function $g(\gamma/\bar{Z})$ is given by,

$$g(\gamma/\bar{Z}) = -[a_1\ (\gamma/\bar{Z})^{3/2}\ [1 + a_2\ (\gamma/\bar{Z})^{1/2}]^{-1/3} \tag{29}$$

with,

$$a_1 = \pi^{1/2}\ [\sum_{i=1}^{\infty} (1 + Z_i)\ \alpha_i\ ]^{-1/2}\ \ [\sum_{i=1}^{\infty} \alpha_i Z_i\ \ (1 + Z_i)]^{3/2}$$

$$a_2 = 2.2\ [\sum_{i=1}^{\infty} \alpha_i Z_i\ \ (1 + Z_i)]^{1/2}\ [\sum_{i=1}^{\infty} (1 + Z_i)\ \ a_i]^{-1/2}$$

The associated lowering of the ionization potential for the transformation of the m-th ion to the (m+1)-th ion is given by Thio[36] as,

$$\Delta V_{m+1} = \frac{e}{4\pi\varepsilon_o} \{\frac{Z_m + 1}{L_D + r_o} + \frac{\bar{Z}^2}{2} [\frac{1}{r_o} f\ (\frac{L_D}{r_o}) - \frac{2}{3(L_D + r_o)}]\} \tag{30}$$

where the function f is given by,

$$f(\varsigma) = 1 - 2\varsigma + 2\varsigma^2 \ln\left(1 + \frac{1}{\varsigma}\right) \tag{31}$$

Saha's equation for the (m+1)-th state of ionization is:

$$\frac{n_{m+1} n_e}{n_m} = 2 \left(\frac{2\pi \, m_e \, k_B \, T}{k^2}\right)^{3/2} \left(\frac{U_{m+1}}{U_m}\right) \exp\left(- \frac{e(V_{m+1} - \Delta V_{m+1})}{k_B \, T}\right. \tag{32}$$

where U_m is the partition function of the ion in the mth state of ionization.

The results developed in this section can now be combined with those of Section 3 to calculate resistivities of real plasmas at a given temperature and pressure, which can be compared with actual experimental measurements. In Figure 2 we show this comparison for high-pressure lithium plasma for which experimental data have been given by Vorobiov[22] for its resistivity as a function of temperature (up to 15000 K) and pressure up to 100 MPa. The agreement with the experimental values are reasonable considering the uncertainty in the experimental data. In the same figure, we have also shown the calculated resistivity for a H plasma as a function of temperature at a specified pressure of 73 MPa, and compared it with the computational result of Kovitya[37]. Again the agreement between the two computed results are reasonable considering the lack of relevant experimental data in this case.

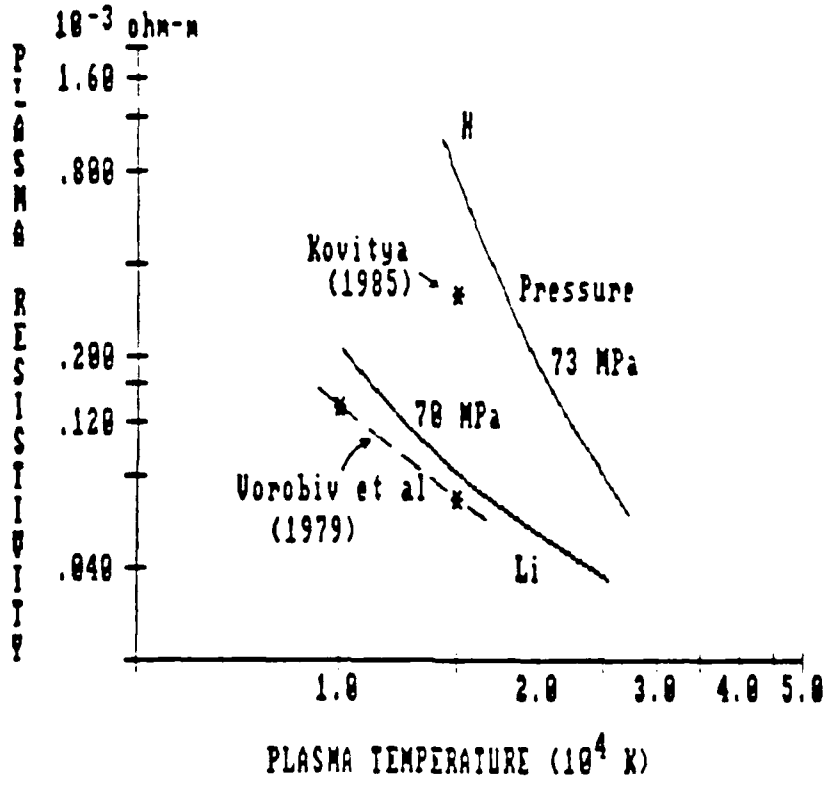

Figure 2 — Resistivity of Li and H plasmas. Comparisons of results of present theory and others.

5. THE MODEL SOLUTIONS AND SCALING RELATIONSHIPS

The main results from the formal solution to the magnetogasdynamic equations can now be assembled as follows:

Dynamical equilibrium: $$I = (2h/\mu w)\ (b_3/b_2)\ T\ I_R^{-2}\ m_A \tag{33}$$

Radiative equilibrium: $$I^2 R_A = 2\ \sigma_s\ g_2\ l\ T^4 \tag{34}$$

Dissipative element: $$R_A = w\ \eta_p / hl \tag{35}$$

Electrical transport: $$\eta_p = g_1\ T^{-3/2} \tag{36}$$

in which,

$$b_3 = (1 + \sum_{i=1}^{\infty} \alpha_i Z_i + g(\gamma/\bar{Z})\ k_B/m_p \tag{37}$$

$$b_2 = \lambda^{-2} \{2\ b_1\ [1 + \lambda^{-1}\ (e^{-\lambda} - 1) - \lambda\} \tag{38}$$

$$b_1 = (\gamma_1^{*} + \tfrac{1}{2})\lambda + 1 \tag{39}$$

$$\lambda = \frac{al}{b_3 T}$$

$$\gamma_1^{*} = \frac{h}{2\mu w} \{L_r^{'} + 2\ \frac{I_a}{I_r}\ M_{12}^{'}\}$$

$$g_2 = \epsilon_r h + \epsilon_i w + (\epsilon_a + \epsilon_b)\ wh/2l \tag{40}$$

$$g_1 = g_{ei} + g_{en} \tag{41}$$

$$g_{ei} = 3.5 \times 10^2 S_T \exp(-\gamma/2\bar{Z}) \tag{42}$$

$$g_{en} = \frac{m_e}{e^2}\left(1 - \sum_{i=1}^{\infty} \alpha_i\right)\left(\sum_{i=1}^{\infty} \alpha_i Z_i\right)^{-1} T^2 \sum_{m=-1}^{\infty} S_m T^{m/2} \tag{43}$$

and l, m_A, T, R_A and η_ρ are the length, mass, temperature, resistance, and resistivity of the plasma armature respectively. I_r is the current flowing through it and the inner rails while I_a is the current in the augmentation windings. L'_r is the inner rails self inductance gradient and M'_{12} is the mutual inductance between the inner rails and the augmentation winding. We have written the relationships (33) - (36) in such a way as to expose the main functional relationship among the principal variables: the plasma armature length l, mass m_A, temperature T, resistance R_A, resistivity η_ρ and the plasma current I_r, where the functional dependence on these variables is strong.

Expressions (33) - (36) can be manipulated to give the temperature, length, resistance and resistivity of the plasma armature in the following forms:

$$\text{Temperature:}\quad T = \left[\frac{\mu\, b_2}{2\, b_3\, m_A}\right]^{4/15} \left[\frac{g_1}{2\,\sigma_s\, g_2}\right]^{2/15} \left(\frac{w}{h}\right)^{2/5} I_r^{4/15} \tag{47}$$

$$\text{Length:}\quad l = \left[\frac{2\, b_3\, m_A}{\mu\, b_2}\right]^{11/15} \left[\frac{g_1}{2\,\sigma_s\, g_2}\right]^{2/15} \left(\frac{w}{h}\right)^{-3/5} I_r^{-6/5} \tag{48}$$

$$\text{Resistance:}\quad R_A = g_1 \left[\frac{\mu\, b_2}{2\, b_3\, m_A}\right]^{1/3} \left[\frac{2\,\sigma_s\, g_2}{g_1}\right]^{1/3} \left(\frac{w}{h}\right) \tag{49}$$

$$\text{Resistivity:}\quad \eta_p = g_1 \left[\frac{\mu\, b_2}{2\, b_3\, m_A}\right]^{-2/5} \left[\frac{g_1}{2\,\sigma_s\, g_2}\right]^{-1/5} \left(\frac{w}{h}\right)^{-3/5} I_r^{-6/5} \tag{50}$$

In general, the R.H.S. of these expressions are implicit functions of the principal variables on the L.H.S. Expressions (47) - (50) serve as a self-consistent set of equations which must be solved simultaneously in order to obtain the structure and properties of the plasma armature. For strongly ionized plasma armatures, the R.H.S. is only very weakly coupled to the variables on the L.H.S., and the above expressions show in an approximate way the explicit dependence of the plasma temperature, length and resistance on the current and the mass of the plasma armature, and on the launcher parameters (L', M' and the bore size). Indeed, in the case of strong ionization, we can show from expressions (33) - (36) that the following is an approximate invariant for the plasma armature according to our model:

$$T^{11}\ j^{-4}\ h^{-2} = \text{constant} \qquad (51)$$

where j is the mean current density in the plasma.

6. RADIATIVE HEAT TRANSFER TO THE WALL

6.1 INTRODUCTION

Gross ablation by the plasma armatures of the wall materials continues to pose a serious problem for railguns to reach high velocity[14] and attain repetitive firing capability[10,13]. The ablation occurs even after the arc has gathered speed from a few hundred meters per second to more than a few kilometers per second.

The phenomenon is a result of many complex processes occuring at the rail-armature and rail-insulator interface. From classical arcs study, the presence of cathode spots and sometimes anode spots are well known[41-45]. In these arc roots, extremely high concentrations of current occur. In many conventional applications of electric arcs in which the mean current density is much smaller than that experienced in railguns, radiation intensity from the arc column (arc interior) is relatively low and insignificant. Under those conditions, the energetic processes in the arc roots dominate the erosion of the electrodes, leading to erosion rates typically in the range of 1 - 100 μg per coulomb of charge transfer.

Unfortunately, this does not appear to be the situation in the case of railgun arcs. Firstly, because of the much higher current density, the mean radiation intensity from the arc body is relatively high. Secondly, the typical erosion rates measured in mass per unit charge transfer observed in railguns is in the range of 10 - 30 mg/C [46], approximately 3 orders of magnitude above those observed in conventional arcs.

In this study we pose a simple but fundamental question: Could the mean thermal flux from the main body of the arc in railguns be sufficient to cause melting, vaporization and hence ablation of the wall materials? If so, what are the key parameters governing this mean thermal flux? Is there a domain of suitable properties and structures for the plasma armature so that ablation caused by the mean thermal flux of the arc could be eliminated?

The present work represents one of a continuing series of efforts to address these issues in a systematic way. It is a significant extension of an earlier study by Powell[7] in that we explore the answers to these questions in a much larger parameter space. It is also extension of an earlier work by Thio[5] in that non-ideal plasma effects are included in the present study.

The dominant contributions to the mean heat flux from the arc are radiation, turbulent thermal conduction and energy generated by hypervelocity skin friction at the wall. It must be noted that the turbulent thermal conduction and skin friction heat generation can be as large or greater than the radiative transfer under certain circumstances[48]. Marshall[40] has recently also drawn attention to the presence of arc roots in railgun arcs. The result of these additional heat transfer mechanisms is to aggravate the wall ablation problem in railguns. An excellent and parallel study, which carefully treats the various forms of energy and momentum transfer to the wall from the arc through the plasma-wall boundary layer, has been completed recently by Tidman, Goldstein and Winsor[48]. In this paper, we shall focus our attention on the radiative contribution.

6.2 THE PHYSICAL FRAMEWORK AND THE METHOD OF ANALYSIS

Consider a stable plasma armature moving at constant acceleration and endowed with a uniform current density, a configuration of minimum peak current concentration for a given total current and spatial extent of the plasma armature. For a given set of gun parameters (such as bore size and rail inductance gradient) and plasma parameters (such

as its total mass and ionic species), using the results developed in Chapter 5, we can calculate the temperature and the length of the plasma armature. The radiative flux from the arc on to the rails and insulators is then determined and this in turn determines the rate of temperature rise in the materials. To this we add the magnetic heating of the rails caused by the pulsed current flowing in them. The length of the plasma armature determines its dwell time at a given position of the wall as it flies by. Together, the radiative heat flux, the rate of thermal energy generation by magnetic heating, and the dwell time determine whether the melting point of the material would be exceeded during the fly-by of the plasma armature.

By appropriately treating the non-ideal plasma behavior in our model, the modelling results should have a higher degree of approximation to the practical situations.

6.3 ARMATURE RESISTANCE, TEMPERATURE, AND LENGTH: AN EXAMPLE

In this section, we present the results obtained directly from the solution of the system of equations (47) - (50), together with the Saha equation (32) and the relevant supporting equations (27) - (31), (37) - (43), for an exemplary case of a railgun which has a 1-cm square bore and an inductance gradient L' of 0.32 μH/m. The calculations are made for currents between 200 kA and 400 kA and unity has been assumed for all emissivities. The scaling factor S_T has been assigned the value of 0.5 which is the value used in obtaining the calibrated resistivity shown in Figure 2.

Figures 3 and 4 show respectively the estimated resistance and temperature of the arc column versus the total number of particles (ions and neutral atoms) in the armature.

When the number of particles is small, say 5×10^{20}, the armature tends to be short, the resistance tends to be high, and the temperature tends to be high.

In the case of a pure Li plasma, the resistance is of the order of 1 mΩ and is relatively insensitive to variation in current. The temperature is relatively high: approximately 25,000 K at a current of

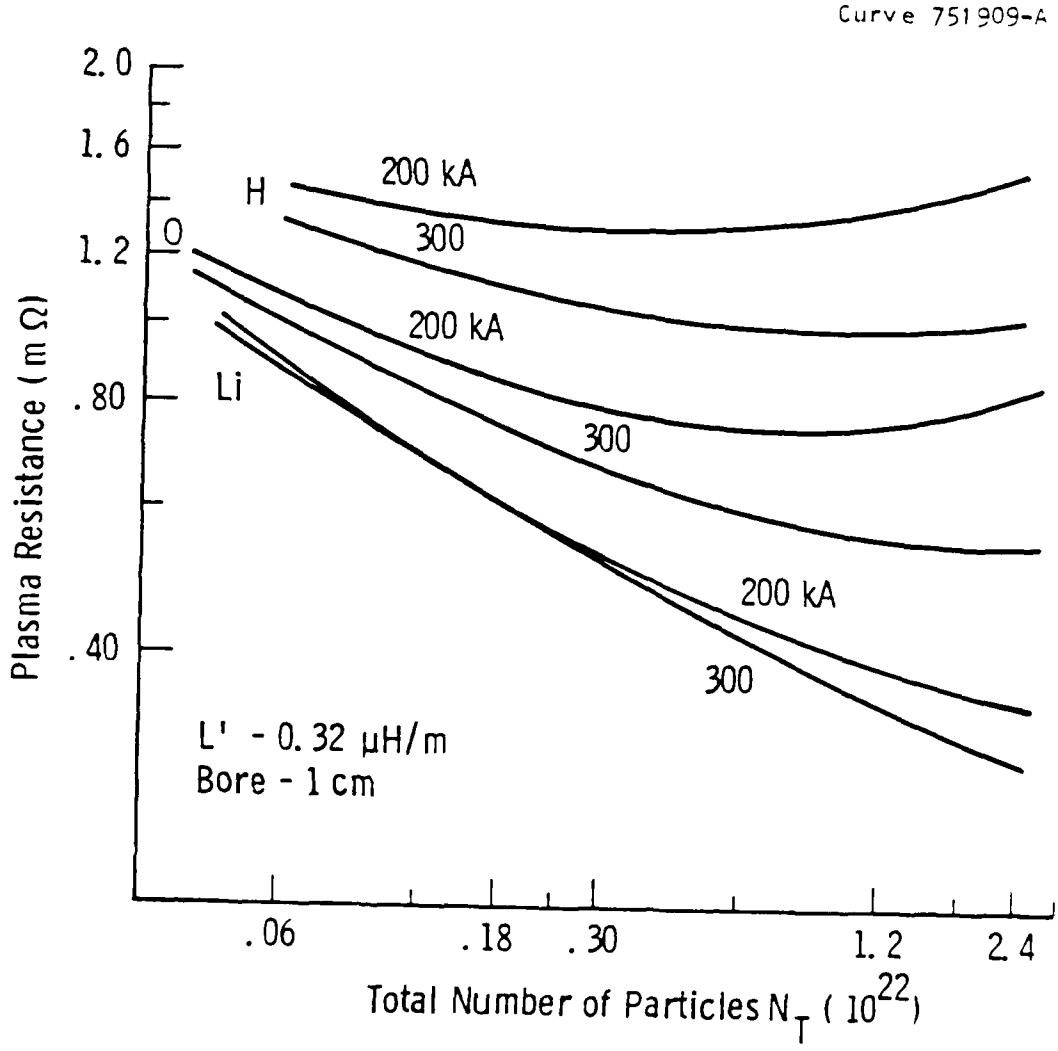

Figure 3 — Arc resistance versus the total number of particles (charged ions and neutrals) in the plasma armature for the case of a railgun with an L' of 0.32 μH/m and a square bore of 1 cm^2 in cross-section.

Curve 751958-A

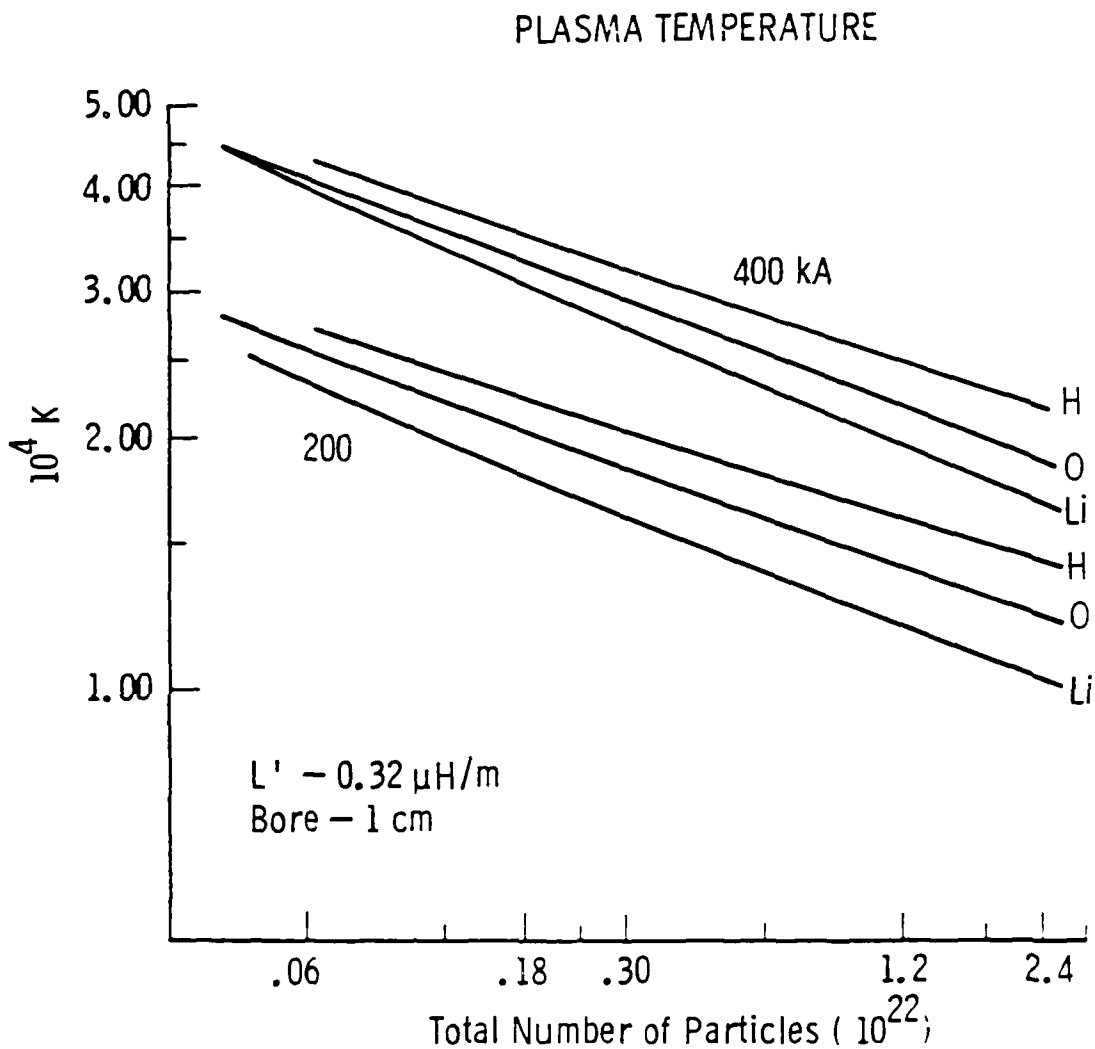

Figure 4 — Temperature of the plasma armature as a function of total number of particles in the armature for the case of a square-bore railgun (1 cm^2) with an L' of 0.32 μH/m.

200 kA and 45,000 K at 400 kA. At these temperatures, the lithium plasma is essentially ideal ($\gamma \ll 0.1$). Thus, the electron-ion contribution of the resistivity here could have been well approximated by Spitzer's expression. Further, due to the relatively low ionization potential of lithium, the Li plasma is nearly fully ionized. Thus the contribution to the resistivity from the electron-neutral scattering is small due to a small concentration of the neutral particles. When these conditions prevail, the net resistance of the armature behaves nearly independently of the current. As the current increases, the temperature increases and the resistivity drops. However, the length of the armature also decreases resulting in a smaller cross-sectional area through which the plasma current passes. The overall effect is to make the net resistance of the armature insensitive to variation in the current.

As the number of particles in the armature increases, the arc length grows, and the resistance generally decreases. In the case of a Li plasma armature in the gun used in the example, the armature resistance is reduced to a level below 0.3 mΩ for a current of 300 kA when the number of particles in the armature reaches a value of 2×10^{22}. However, the plasma also cools with increasing number of particles. In the case of H or O plasma, due to the high ionization potential of the atomic species, the degree of ionization in these plasmas decreases rapidly as the plasma cools. The consequence is the presence of a high concentration of neutral particles giving rise to a significant contribution from the electron-neutral scattering to the resistivity and consequently a higher resistance. Thus in these plasmas, the overall armature resistance at first decreases with the number of particles present in the armature until a point is reached when further increase in the number of particles makes the neutrals dominate the plasma resistivity. Beyond that point, the armature resistance increases with increasing number of particles.

For a pure O plasma at 300 kA, the resistance decreases from approximately 1.2 mΩ for 5×10^{20} particles to about 0.6 mΩ for 1×10^{22} particles in the armature. For a pure H plasma at the same current, the resistance appears to fall from 1.4 mΩ to 1 mΩ as the number of particles is increased from 5×10^{20} to 1×10^{22}. When the number of particles increases beyond 2×10^{22}, the armature resistance begins to gradually increase.

With reference to Figure 4 and 5, we see that the armature temperature and more importantly the radiation intensity decreases monotonically with increasing number of particles.

At 200 kA when the number of particles increases from 5×10^{20} to 2×10^{22} the temperature of a Li plasma drops from 25,000 K to 12,000 K. The corresponding radiation intensity from the armature falls from 2.5 MW/cm^2 to below 0.1 MW/cm^2. For an O plasma armature, the temperature decreases from approximately 27,000 K to about 13,000 K and the radiation intensity goes from 3 MW/cm^2 to about 0.14 MW/cm^2. For a H plasma armature, the temperature decreases from about 30,000 K to about 20,000 K and the radiation intensity drops from about 5 MW/cm^2 to approximately 0.25 MW/cm^2.

At 400 kA, when the number of particles increases from 5×10^{20} to 2×10^{22}, the temperature of a Li plasma drops from a 45,000 K to 18,000 K. The corresponding radiation intensity from the armature falls from 25 MW/cm^2 to below 0.5 MW/cm^2. For an O plasma armature, the temperautre decreases from approximately 45,000 K to about 20,000 K and the radiation intensity goes from 25 MW/cm^2 to about 0.8 MW/cm^2. For a H plasma armature, the temperature decreases from about 47,000 K to about 23,000 K and the radiation intensity drops from about 30 MW/cm^2 to approximately 1 2 MW/cm^2.

Even refractory and conducting materials such as tungsten or molybdenum are unable to survive the radiation from the armature for more than a few μs when the radiation intensity exceeds 5 MW/cm^2. For radiation intensity below 1 MW/cm^2, there is a chance for these materials to survive if the dwell time of the plasma armature is of the

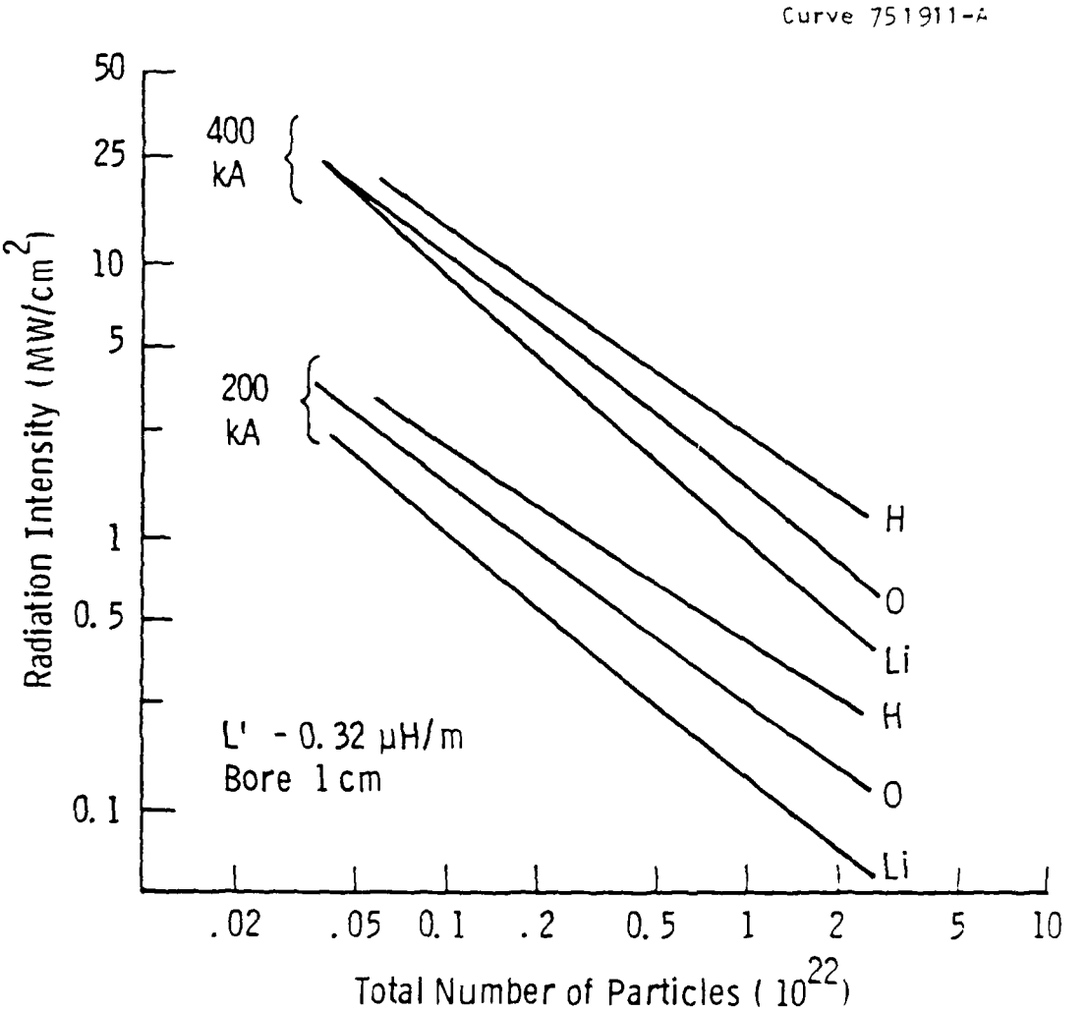

Figure 5 — Radiation versus total number of particles in the plasma armature for the case of a square-bore railgun with a bore cross-section of 1 cm^2 and an L' of 0.32 μH/m.

order of tens of μs. The thermal conductivity of the materials plays an important part. In the next section, the radiative heating of the wall materials is analysed.

6.4 PLASMA RADIATIVE HEATING OF THE WALL MATERIALS

The wall of the bore is subjected to an incident radiative flux given by,

$$Q = \epsilon \sigma_s T_A^4 \tag{52}$$

where T_A is the arc temperature, σ_s is the Stefan constant, and ϵ the effective emissivity. We shall assume unity for the effective emissivity for want of exact experimental data. This will tend to overestimate the radiative flux. The temperature T_A strictly should be the temperature of the arc at a point which is approximately one optical (Rosseland) path length from the wall. Again, we can obtain a worst-case estimate by using the arc column temperature calculated from the model as the value for T_A.

Before the onset of melting, the wall temperature increases according to the standard equation for heat conduction in solid,

$$\rho c_v \frac{\partial T}{\partial t} = \frac{\partial}{\partial x} \left(\kappa \frac{\partial T}{\partial x} \right) \tag{53}$$

where ρ is the mass density, c_v is the specific heat per unit mass of the rail, κ is its thermal conductivity, and x is the displacement into the wall perpendicular to its surface. The boundary condition at the wall surface (x = 0) providing the radiative heat flux is,

$$\frac{\partial T}{\partial x} = - Q = - \epsilon \sigma_s T^4 \tag{54}$$

Equation (53) with the boundary condition (54) can be solved to give the temperature at a point x and time t to be,

$$T(x,t) = T_o + Q\,\{(\pi\lambda)^{-1}\exp(-\lambda^2 x^2) - x\,\mathrm{Erfc}(\lambda x)\}/\kappa \qquad (55)$$

$$\lambda = (\rho\, c_v/4\kappa t)^{1/2}$$

where T_0 is the initial temperature of the rail. At the rail surface, $x = 0$, the temperature at time t is,

$$T(0,t) = T_0 + 2\,Q\,(t/\pi\rho c_v\kappa)^{1/2},\quad t<t_r \qquad (56)$$

In the above, the time t is measured from the instant the plasma armature first reaches the point of interest. The above expression applies only during the fly-by of the plasma armature. The dwell time of the plasma is indicated as t_r. After this time, the wall temperature would then fall off. It can be shown that, after the armature fly-by, the surface temperature of the wall at time $t > t_r$ is given by

$$T(0,t) = T_0 + 2\,Q\,\{t^{1/2} - (t - t_r)^{1/2}\}/(\pi\rho c_v\kappa)^{1/2} \qquad (57)$$

The above heating of the wall by the plasma radiation applies to both the rail and the insulator. For the rail, an additional heating mechanism needs to be included: the magnetic heating (or commonly called Joule heating) of the rails. The magnetic and radiative heating of the rails strictly are a coupled thermal process. In a recent paper, Powell[7] treats this coupled phenomenon by carefully formulating a 1-D model in which the equations governing the velocity-skin effect (magnetic) heating of the rail is solved simultaneously with the equations for the radiative transfer. As also noted by Powell, there exists at present a high degree of uncertainty between application of the theoretical results and interpretations of experimental observations in any exact form. In view of this uncertainty, it appears that a consistent degree of accuracy can still be obtained even if we seek a simplification of the mathematical problem by un-coupling the magnetic

heating of the rail from the radiative heating. In this procedure, we adopt a worst-case approach in estimating the heating effects from each of these contributions. By treating the combined effects as a superposition of the separate effects, the overall estimate for the temperature rise in the rails can reasonably be expected to be conservative in the maximal sense. This simplification allows rapid parametric studies over a wide range of plasma and rail parameters to be performed. The approach is in essence equivalent to a lump-parameter method.

6.5 MAGNETIC (OR JOULE) HEATING OF THE RAILS

The precise way of taking account of magnetic heating of the rails is to solve the coupled set of partial differential equations governing strong magneto-thermal diffusion in a conductor,coupled to the electrodynamics of the moving arc. An upper bound to the temperature rise due to magnetic heating, however, can be obtained as follows. The magnetic field within the plasma armature decreases from the breech-end of the armature to the muzzle-end of the armature according to the uniform current density model developed above. During the fly-by of the plasma armature, at a given station on the surface of the rail, one would see a magnetic field increasing monotonically with time. In the case of an uniform current density model, this monotonicity degenerates into one of linearity. After the plasma armature has completely passed by, the magnetic field takes on the value of the field produced by the constant current flowing in the rails. The temperature rise due to this temporal monotonic increasing variation of magnetic field with a plateau amplitude after a certain lapse of time is always less than that due to a sudden switch-on of a magnetic field with the same plateau amplitude. For a conservative (maximal) estimate of the rail surface temperature due to Joule heating, we may therefore use the result for the case of a sudden switch-on of a magnetic field.

For the sudden switch-on of a magnetic field, the peak temperature rise occurs at the conductor surface and at the instant of

switching on the field, if effects associated with temperature-dependent material properties were neglected.

The question remains whether 2-D or even 3-D effects are important in determining the magneto-diffusion heating effects in the case of finite and curved rails. It can be shown that, in a sufficiently short time scale and in a sufficiently thin layer of the rail closed to the surface, 2-D or 3-D magneto-diffusion may be ignored. In particular, the peak surface temperature which occurs at t = 0 may be obtained from a solution of a 1-D magneto-diffusion problem:

$$\mu \frac{\partial H}{\partial x} = \frac{\partial}{\partial x}\left(\eta \frac{\partial H}{\partial x}\right)$$
$$\rho c_v \frac{\partial T}{\partial t} = \frac{\partial}{\partial x}\left(\kappa \frac{\partial T}{\partial x}\right) + \eta \left(\frac{\partial H}{\partial x}\right)^2 \tag{58}$$

with the appropriate boundary conditions, where μ is the magnetic permeability, η is the rail resistivity and the other symbols have their usual meaning. Again, locally and for the very short time of interest, the boundary conditions can be chosen to be the same as those for a semi-infinite conducting half-space, with the surface of the half-space corresponding to the rail surface. The problem now reduces to one originally solved by Kidder[49] and analyzed by several other investigators, e.g.[47]. From their solution, the maximum surface temperature rise can be given as,

$$\Delta T = \frac{4}{\pi \rho c_v}\left(\frac{1}{2}\mu H_o^2\right) \ln\left[1 + \frac{\pi}{2}\left(\frac{\rho c_v \eta}{2\mu\kappa}\right)^{1/2}\right] \tag{59}$$

We use this expression to provide the upper bound to the magnetic heating of the rail due to the moving plasma armature.

6.6 MINIMUM ARMATURE VELOCITY FOR WALL SURVIVABILITY

If the plasma armature enters a barrel section with an entry velocity v_0 and is subjected to a constant acceleration a, the dwell time t_r of the armature at the entry point is given by,

$$t_r = \{(v_0^2 + 2al)^{1/2} - v_0\}/a \tag{60}$$

where l is the length of the plasma armature which is obtained from solving the plasma model as described by Chapter 5. For a constant acceleration, the armature dwell time decreases with increasing entry velocity v_0. In the case of the rail, the total temperature rise is given by,

$$\Delta T_{rail} = T_r + T_j \tag{61}$$

where T_r is the temperature rise due to radiative heating given by expression (56), and T_j is the temperature rise due to Joule (magnetic) heating given by expression (59). In the case of insulator, the total temperature rise consists of only the radiative term. From expression (56), we see that the total temperature rise of the wall decreases with decreasing armature dwell time. In order to control the wall temperature rise to be below a certain specified value, the armature dwell time is required to be below a certain value. In turn, this requires a certain entry velocity for a given acceleration of the armature. Substituting expression (60) for the dwell time in the radiative heating expression (56), and introducing the resultant expression in (61) and using the Kidder's temperature expression (59), if necessary, in expression (61), an equation is obtained for the minimum entry velocity for a given acceleration, or a minimum acceleration for a given entry velocity.

Let T_m be the melting point of the wall material and T_0 its initial temperature. The maximum allowable temperature rise at the wall surface before onset of melting is given by $\Delta T = T_m - T_0$. In practice,

because of thermal softening of the wall material at elevated temperature and the requirement to withstand the high pressure of the plasma armature, the allowable temperature rise for the wall is considerably lower than is given by the above expression (based upon the melting point) in order to avoid significant damage of the wall material.

Figure 6 shows the result of solving the resultant equation for minimum entry velocity to control the temperature rise in the tungsten rails to below 2500 K for a railgun with 1-cm square bore, 0.32 μH/m, and a 1-g projectile. The calculations are made for the 3 different single-element plasmas, Li, O and H, and for different values of current, 200 kA and 300 kA. The minimum entry velocity is shown versus the total number of particles in the armature.

At 300 kA for this gun, the required velocity for the armature to avoid rail damage can be seen to be very high (exceeding 50 km/s) for all the 3 different plasmas when the armature contains less than 10^{21} particles. Only when the armature contains more than 10^{22} particles does the minimum armature velocity fall below 20 km/s in the case of a H plasma armature, and below 10 km/s in the case of an O plasma. In the case of a Li plasma, the calculation indicates that an entry velocity as low as 1 km/s would be sufficient to avoid radiative damage if more than 10^{22} particles are present in the plasma armature.

At 200 kA, the situation improves markedly. With more than 10^{22} particles in the armature, the tungsten rails appear to be able to survive the armature radiation for moderate armature velocity for all the 3 different plasmas. Specifically, for a H plasma a minimum armature velocity of approximately 5 km/s is required, and for both O and Li plasmas, an entry velocity of the order of 100 m/s appears to be all that is neccessary to avoid radiative damage. On the other hand, if only 10^{21} particles are used, entry velocity of 8 km/s, 10 km/s, and 20 km/s are required for a Li, O and H plasma armature respectively.

6.7 CONCLUSION

On the one hand, the modelling results show that arc radiation is sufficiently high to cause ablation under the conditions of most

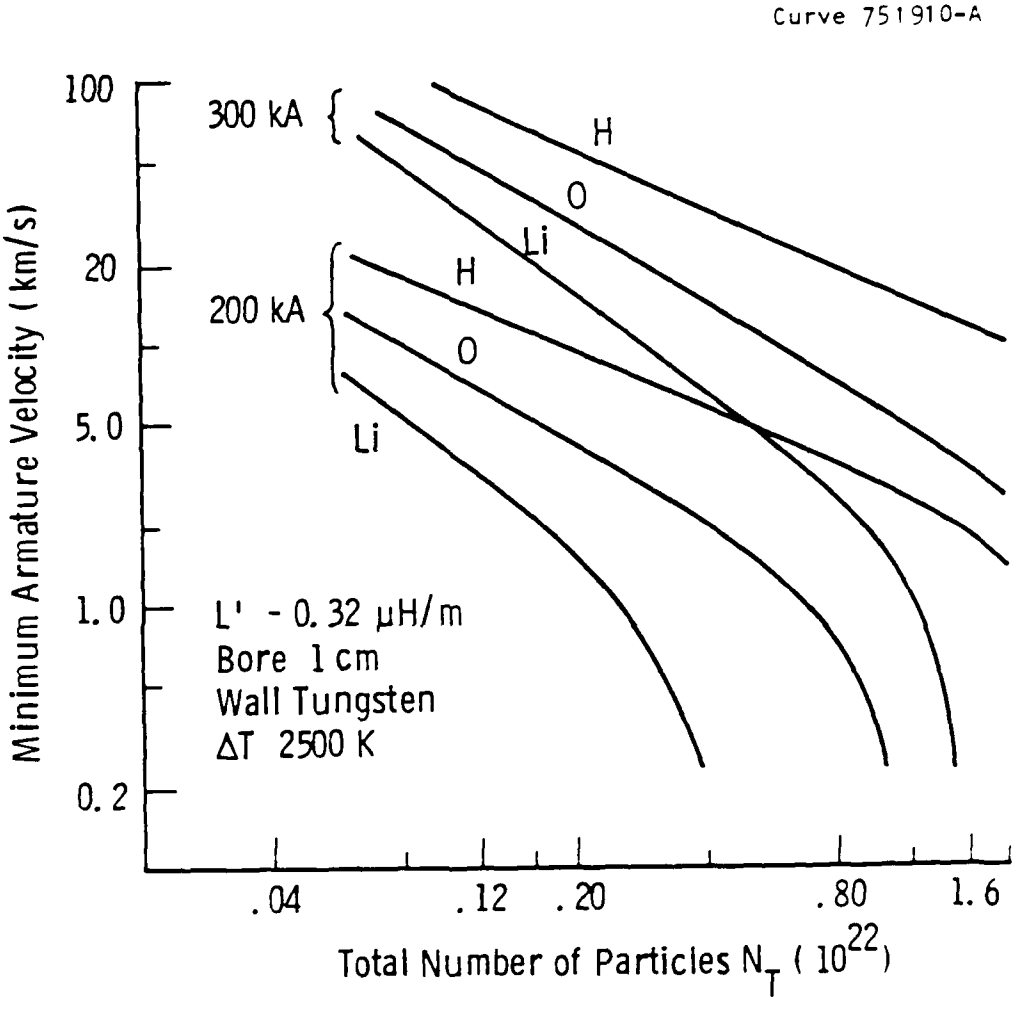

Figure 6 — Minimum armature velocity to limit the temperature rise in a tungsten rail to below 2500 deg K_2 for a square-bore railgun with a bore cross-section of 1 cm^2 and a L' of 0.32 μH/m.

railgun experiments conducted in the past. Under the same conditions the arc also tends to have a rather high resistance (above 1 mΩ). These properties were a consequence of operating the plasma armature under less than optimum conditions. In particular, the plasma armatures in these experiments were initiated with less than the required number of particles to prevent radiative ablation. As a result, the initial plasma is very hot, emits radiation at a high intensity, and begins to ablate the wall materials. Also, because of insufficient number of particles, the arc has a short length giving rise to a high resistance. On the other hand, the modelling results indicate that there indeed exist domains of operating parameters in which radiative ablation of the wall materials can possibly be eliminated. For a given set of gun parmeters and a given current, we can generally find a combination of number of particles in the armature and the armature velocity by which radiative ablation would not occur. We find, indeed, that by using a low atomic weight, low ionization potential ionic species such as Li, the armature velocity could be as low as a few km/s when radiative ablation can be totally avoided under typical railgun operating conditions, and that the mass of the lithium armature required to initiate the arc remains below 10% of the projectile mass. In general, a large number of particles are required to produce a sufficiently cool plasma. The greater length of the resulting armature in general also tends to lower its electrical resistance.

Whether such armatures can be conveniently produced and maintained throughout the launch remains a development for the future. Further, the greater length for the armature could possibly increase the overall viscous drag, and the lower conductivity of the cool plasma could possibly lead to weaker coupling between the magnetic field and the plasma. Both effects could contribute to its instability. Preliminary investigations on these issues have been made on the related program[16]. Much more theoretical and experimental research on these issues are needed.

7. ACKNOWLEDGEMENT

This work was done primarily with the sponsorship of the U.S. Army Research Office under contract DAAG29-83-C-0030. In parts it has also been supported by a companion program sponsored by the Department of Energy under contract DE-AC02-83ER13048.

8. REFERENCES

1. I. R. McNab, "Electromagnetic Macroparticle Acceleration by a High Pressure Plasma", J. Appl. Phys., 51, pp. 2549-2551, 1980.

2. J. D. Powell and J. H. Batteh, "Arc Dynamics in the Rail Gun", J. Appl. Phys., 52, pp. 2717, 1981. Also, IEEE Trans. Magnetics, Vol. MAG-18, Jan 1982, pp. 7-10.

3. Y. C. Thio, "Electromagnetic Propulsion of Matter to Hypervelocity", 6th Int. Symposium in Ballistics, Orlando, Florida, American Defense Preparedness Association, Oct 27-29, 1981.

4. Y. C. Thio, "PARA: A Computer Simulation Code for Plasma Driven Electromagnetic Launchers", Report MRL-R-873, Materials Research Laboratories, DSTO, Maribyrnong, Melbourne, Victoria, Australia, March 1983.

5. Y. C. Thio, I. R. McNab and W. C. Condit, "Theoretical Performance of Plasma Driven Railguns", Paper AIAA-83-1751, American Institute of Aeronautics and Astronautics, 1983.

6. J. D. Powell and J. H. Batteh, "Two-Dimensional Plasma Model for the Arc-Driven Rail Gun", J. Appl. Phys., Vol. 54 (5), 1983, pp. 2242-2254.

7. J. D. Powell, "Thermal Energy Transfer from Arc to Rails in An Arc-Driven Rail Gun", IEEE Trans. Magnetics, Vol. MAG-20, Mar. 1984, pp. 395-398.

8. J. H. Batteh, "Momentum Equation for Arc-Driven Rail Guns", J. Appl. Phys. Vol 56 (11), Dec. 1984, pp. 3182-3186.

9. R. S. Hawke, A. L. Brooks, F. J. Deadrick, J. K. Scudder, C. M. Fowler, R. S. Caird and D. R. Peterson, "Results of Rail-gun Experiments Powered by Magnetic Flux Compression Generators", IEEE Trans. Magnetics, MAG-18, 1982, pp. 82-93.

10. Y. C. Thio, G. A. Clark and A. J. Bedford, "Results from an Experimental Railgun System: ERGS-1A", Report MRL-R-875, Materials Research Laboratories, Defence Science & Technology Organization, Maribyrnong, Melbourne, Australia, March 1983.

11. A. J. Bedford, G. A. Clark and Y. C. Thio, "Experimental Electromagnetic Launchers at MRL", Report MRL-R-894, Materials Research Laboratories, DSTO, Maribyrnong, Melbourne, Australia, August 1983.

12. G. A. Clark and A. J. Bedford, "Performance Results of a Small-Calibre Electromagnetic Launcher", IEEE Trans. Magnetics, MAG-20, Mar. 1984, pp. 276-279.

13. A. J. Bedford, "Rail Damage in a Small Callibre Rail-Gun", IEEE Trans. Magnetics, MAG-20, Mar. 1984, pp. 245-251.

14. J. Parker, W. M. Parsons, C. E. Cummings, and W. E. Fox, "Performance Loss due to Wall Ablation in Plasma Armature Railguns", Paper AIAA-85-1575, AIAA 18th Fluid Dynamics, Plasmadynamics and Laser Conference, July 16-18, 1985, Cincinatti, Ohio.

15. L. Patch, J. M. Comstock, Y. C Thio, and F. J. Young, "Rail-gun Barrel Design and Analysis", IEEE Trans. Magnetics, Vol. MAG-20, Mar. 1984, pp. 360-363.

16. Y. C. Thio, W. C. Condit, T. J. Dougherty, D. L. Ometz, N. A. Ottinger, P. L. Ulerich, D. M. York and J. M. Zomp, SUVAC Annual Report I, 1984.

17. A. H. Khalfaoui, "Electrical Conductivity of Nonideal Quasi-Metallic Plasmas", IEEE Trans. Plasma Sci., PS-12 (3), Sept. 1984, pp. 179-191.

18. Yu. K. Kurilenko and K. K. Valuev, "The Electrical Conductivity of Plasma in the Wide Range of Charge Densities", Beitr. Plasmaphys., 24 (3), 1984, pp. 161-172.

19. I. Ya. Dikhter, V A. Zelgarnik, and S. V. Smagin, "Electrical Conductivity of a Dense Strongly Ionized Alkali Metal Plasma", High Temperature, 17(2), 1979, pp. 217-221.

20. V. V. Vorobiov, P. P. Kulik, A. V. Pallo, A. A. Rakitin, E. K. Rozanov and V. A. Riabyi, "Experimental Investigation of The Electrical and Heat Conductivities of Alkali Dense Plasmas", Journal de Physique, Coll. C7, Supplement 7, Tome 40, 1979, pp. 693-694.

21. V. A. Alekseev and I. T. Iakubov, "Non-Ideal Plasmas of Metallic Vapours", Phys. Rep., 96(1), 1983, pp. 1-69.

22. H. A. Bethe and R. Jackiw, Intermediate Quantum Mechanics. 2nd Ed. Reading, Massachusetts: Benjamin, 1968.

23. L. S. Frost, "Conductivity of Seeded Atmospheric Pressure Plasmas", J. Appl. Phys., Vol. 32, pp. 2029-2036, 1961.

24. A. B. Cambel, Plasma Physics and Magnetofluid-Mechanics. New York: McGraw-Hill, 1963.

25. D. A. Liberman, "INFERNO: A Better Model of Atoms in Dense Plasmas", J. Quant. Spectrosc. Radiat. Transfer, Vol 27 (3) pp. 335-339, 1982.

26. G. I. Kerley and J. Abdallah, Jr., "Theoretical Equations of State for Molecular Fluids: Nitrogen, Oxygen, and Carbon Monoxide", J. Chem. Phys., Vol. 73 (10), pp. 5337, 1980.

27. G. Rinker, The Electrical Conductivity of an Arbitrarily Dense Plasma", Report LA-9872-MS UC-34, Los Alamos National Laboratory, New Mexico, 1984.

28. R. D. Cowan and J. Ashkin, Phys. Rev., Vol 105, p. 144, 1957.

29. K. S. Holian, Editor. T-4 Handbook of Material Properties Data Bases. LA-10160-MS, Los Alamos National Laboratory, Los Alamos, NM, 1984.

30. A. Unsold, Z. Astrophys., 24, p. 355, 1984.

31. G. Ecker and W. Kroll, "Lowering of Ionization Energy for a Plasma in Thermodynamic Equilibrium", Phy. Fluids, Vol. 6 (1), pp. 62-69.

32. R. J. Rosado, D. C. Schram and J. Leclair, "Continuous emission, lowering of the ionization potential and total excitation cross-sections of an atmospheric thermal plasma", J. Phys., Colloq. C7 (Orsay, France), 1979, pp. 285-286.

33. S. K. Srivastava and G. L. Weissler, "The lowering of the spectral series limit of hydrogen and carbon in a plasma", IEEE Trans. Plasma Sci., Vol. 1 (4), pp. 17-22, 1973.

34. H. Ehrich and H. J. Kusch, "Lowering of the ionization potential of Carbon II ions in a high-pressure plasma", Z. Naturforsh., Teil A, Vol. 29 (5), 1974, pp. 810-818. 34. L. D. Landau and E. M. Lifshitz, Statistical Physics, Reading, Mass.: Addison-Wesley, 1958.

35. Ya. B. Zel Dovich and Yu. P. Raizer, "Physics of Shock Waves and High-Temperature Hydrodynamic Phenomena", Vol. I and II, Academic Press, New York, 1966.

36. Y. C. Thio, "A Simple Expression for Pressure and Ionization Energy Correction for a Non-Ideal Plasma", To be submitted for publication.

37. P. Kovitya, "Physical Properties of High-Pressure Plasmas of Hydrogen and Copper in the Temperature Range 5000-60000 K", IEEE Trans. on Plasma Science, Vol. PS-13, No. 6, December 1985, pp. 587-594.

38. D. F. Stainsby and A. J. Bedford, "Some diagnostics interpretations from railgun plasma profile experiments", IEEE Trans. Magnetics, Vol. MAG-20, No. 2, 1984, pp. 332.

39. R. A. Marshall, "Plasma puffing from a railgun armature", ibid pp. 264.

40. R. A. Marshall, "Structure of plasma armature of a railgun", Proc. 3rd Symposium on Electromagnetic Launch Technology, April 20-24, 1986, Austin, Texas, pp. 165-168. (41)

41. E. Hantzsche, "Estimation of the Current Density in Cathode Arc Spots", Contrib. Plasma Phys., 25 (5), 1985, pp. 459-465.

42. E. Hantzsche and B. Juttner, "Current density in arc spots", IEEE Trans. Plasma Sci., Vol PS-13, No. 5, 1985, pp. 230-234.

43. S. Anders, B Juttner, H. Pursch, and P. Siemroth, "Investigations of the Current Density in the Cathode Spot of a Vacuum Arc", Contrib. Plasma Phys., 25 (5), 1985, pp. 467- 473.

44. G. Ecker, "Unified Analysis of the Metal Vapour Arc", Z. Naturforsch., 28 a, 1973, pp. 417-428.

45. J. D. Cobine and E. E. Burger, "Analysis of electrode phenomena in the high-current arc", J. App. Phys., 26 (7), pp. 895-900, 1955.

46. R. F. Askew, B. A. Chin, B. J. Tatarchuk, J. L. Brown, and D. B. Jensen, "Rail and insulator erosion in rail guns", Proc. 3rd EML Technology Symposium, April 20-24, 1986, pp. 1- 5.

47. R. S. Hawke and J. K. Scudder, "Magnetic Propulsion Railguns: Their Design and Capabilities," in Megagauss Physics and Technology, P. J. Turchi, ed., Plenum Press, New York, 1980, pp. 297-312.

48. D. A. Tidman, S. A. Goldstein and N. K. Winsor, "A Rail Gun Plasma Armature Model," Paper submitted for publications in IEEE Transactions on Magnetics, April, 1986.

49. R. E. Kidder, Lawrence Livermore National Laboratory, Livermore, California, 1960.

END

DTIC

7-86